Automated Guided Method for Roadheader fuselage

Hongyue Chen
Liaoning Technical University
Wei Yang (aygxy_yw130@163.com)
Liaoning Technical University https://orcid.org/0000-0002-9106-7504
Desheng Zhang
Tiandi Science and Technology Co., Ltd.
Song Xiao
Shannxi Yanchang Petroleum Balasu Coal Industry Co., Ltd.

Research

Keywords: Motion control, Prediction model, Path planning, Roadheader

Posted Date: June 1st, 2021

DOI: https://doi.org/10.21203/rs.3.rs-558698/v1

Automated Guided Method for Roadheader fuselage

Hongyue Chen[1], Wei Yang[1,2*], Desheng Zhang[3], and Song Xiao[4]

[1]*Liaoning Technical University, Fuxin 123000,China*

[2]*Anyang Institute of Technology, Anyang 455000,China*

[3]*Tiandi Science and Technology Co., Ltd., Beijing 100000, China*

[4]*Shaanxi Yanchang Petroleum Balasu Coal Industry Co., Ltd., Yanchang 717100, China*

Corresponding author: Wei Yang (e-mail: aygxy_yw130@ 163.com).

Abstract：Autonomous Navigation of roadheader is a hot topic in recent research. The subject of this paper mainly focuses on the motion control of the roadheader fuselage. Because of the particularity of its work content and operational environment, the motion control is different from that of the traditional differential-drived vehicle. This paper introduces a method to detect the position and posture of roadheader fuselage in harsh underground environment, which lays a foundation for motion control. In addition, a path planning method based on prediction model is proposed to reduce the control effort while ensuring enough control accuracy. Then the kinematics characteristics of roadheader fuselage with and without the path planning process are analyzed and compared by simulation. The result shows that the proposed method makes the movement of the roadheader smoother and more suitable for the tunneling process compared with the conventional method.

Keywords： Motion control, Prediction model, Path planning, Roadheader

1 Introduction

Automatic tunneling is of great significance to improve the excavation efficiency and reduce the labor of workers (Wang et al. 2019; Wang et al. 2018). As the roadheader is the core equipment for tunneling, the automatic control of roadheader is the premise of automatic tunneling (Wang et al. 2017). A roadheader can be regarded as a tracked vehicle so called fuselage on which a cutting mechanism loaded. Thus, the automatic control of roadheader includes two issues, the automated guided control of the tracked vehicle (i.e. the fuselage) and movement control of the cutting mechanism joint. Our work mainly focuses on the former.

For the motion control of roadheader, the fuselage pose should be firstly detected because it provides necessary reference parameters in the control process. However, it is not an easy task due to the poor GPS signals, strong vibration, high dust and other adverse factors in the tunnel. The traditional methods, including inertial navigation (Tian et al. 2019), iGPS (Tao et al. 2015), radar scanning (Zhao. 2011), UWB based local positioning (Fu et al. 2015) method cannot work well in the harsh underground environment. A laser guided method (Li. 2012) is used for the pose detection of the fuselage in this paper. This method originates from the present wide-used device called laser orientation instrument. The improvement is that the transmitter is replaced by a device which can generate a laser plane as a measurement reference. At the same time, photoelectric sensors are mounted on the fuselage to receive the laser information. As the fuselage deviate from the expected pose, the sensed data of photoelectric sensors vary with the change of the fuselage pose. Then the pose can be calculated based on the sensed data.

Then we step to the motion control issue. At present, the algorithms in common usage include PID feedback control, pure pursuit tracking algorithm, predictive following algorithm and Stanley method. PID control is a simple and effective method widely used in industry. However, it is difficult to apply to multivariable systems or time-varying systems (Moshayedi et al. 2019). The implementation of pure

pursuit tracking algorithm is described in reference (Coulter. 1992), including the geometric derivation of the method, and the influence of some key parameters on the performance of the algorithm. The application of pure pursuit tracking algorithm in reactive tracking path is studied in reference (Morales et al. 2009) and experiments are carried out with tracked mobile robot in indoor environment. It is proved that the controller has reliable and smooth path tracking characteristics. Preview tracking algorithm is to detect forward in the process of driving, so as to imitate the real driving of the driver (Hu et al. 2019). The vehicle can detect the change of the forward path ahead of time and use it as an optimization goal to adjust the angle ahead of schedule. The algorithm can reduce the fluctuation of lateral displacement and heading angle, and make the vehicle move more smoothly. The Stanley method (Skakauskas et al. 2021) used by Stanford University unmanned vehicle is a nonlinear feedback function based on cross track error, and can realize the exponential convergence of the cross track error to zero. This method is based on the front axle control algorithm of wheeled vehicle platform, which is not suitable for differential driven tracked vehicle.

For the motion control of the roadheader fuselage, additional factors should take account into, including the width of the tunnel, the operation range of cutting mechanism, and even the process flow of tunneling excavation. Compared with common automated guided vehicle issue, the motion control of roadheader has the following remarkable features.

First, it is a point-to-point control problem rather merely a trajectory tracking problem. The reason is as follows. According to the excavation process, the roadheader needs move from last working position (i.e. start point) to the next working position (i.e. goal point) where the cutting mechanism cuts the coal wall. Note that the cutting mechanism does not work when the fuselage is walking forward, the tunnel section accuracy will not be affected by the deviation of fuselage during the moving stage. So what should be ensured is the pose and position accuracy of the fuselage at the working position rather that of each point on the path.

Second, the control strategy contains two steps, path planning and trajectory tracking. Formerly, it is thought that the path has been determined, that is, the middle line of tunnel (Zhang et al. 2021). However, as mention above, for a point-to-point control problem, the first thing we should do is to plan the path between the start point and the goal point.

Third, the kinematic characteristics of the moving vehicle are different. The speed of a normal vehicle is fast, while the walking speed of roadheader is very slow, even less than 0.1 m/s. For low-speed vehicle trajectory tracking, the motion control algorithm based on kinematics works well. Relatively, the weight of the roadheader is huge, generally 60 - 100 tons. Therefore, the control effort should be reduced as much as possible to avoid excessive burden on the drive system.

This paper proposed a path planning strategy based on the goal point prediction, which takes the predetermined point as the tracking target to plan the path of the roadheader. The strategy tries to reduce the control effort and meanwhile maintain the position and heading accuracy of the roadheader at the goal point.

The remainder of this paper is organized as follows: Section 2 introduces the overall scheme of the control system. Section 3 introduces the pose detection method. Section 4 introduces the motion control method. Section 5 introduces the simulation experiments. Section 6 summarizes the whole paper and draws a conclusion.

2 Overall Design

The system consists of two subsystems, pose detection system and motion control system. The former is used to detect the pose and position of the roadheader relative to the tunnel, and the latter is used to correct the movement of the roadheader fuselage to make sure the position and attitude are as expected at the working position. Fig. 1 shows the overall design. The data interaction module is used to communicate with the computer and transmit the measurement data of the sensors. The pose and motion state of the

roadheader fuselage are compared with that of the expected in real time to obtain the pose error. Then the required adjustment is calculated according to the preset control strategy. DSP controller is used to send control instructions to the hydraulic system through D/A conversion module, and the movement speed of left and right tracks are changed by adjusting the flow of hydraulic system.

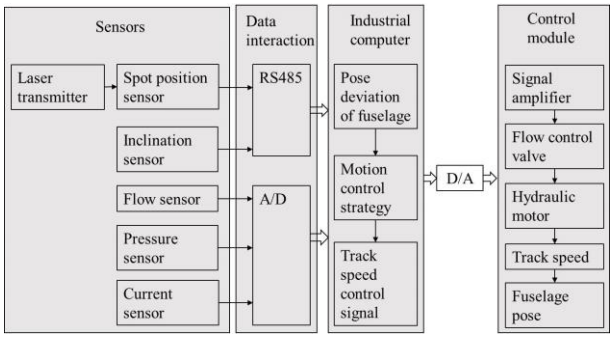

Fig. 1 Overall design of motion control system

3 Pose detection method

The pose detection system deploys a laser transmitter, several photoelectric sensors and an inclination sensor. Fig. 2 shows the layout of all the devices involved. The laser transmitter can generate a planar laser which is used as a measurement reference. Photoelectric sensors mounted on the fuselage can measure the position where the laser incidents on, that is, the location of the laser spots. The inclination sensor can measure the pitch angle and roll angle of the fuselage. Based on all the sensed data, the key pose parameters, lateral offset and yaw angle can be calculated by attitude matrix.

$$\alpha = \arctan\frac{(d_1-d_2)\cos\gamma - H\sin\gamma}{(d_1-d_2)\sin\beta\sin\gamma - L\cos\beta + H\sin\beta\cos\gamma} \tag{1}$$

$$\begin{aligned} y = &-d_1(\mathrm{c}\alpha\,\mathrm{c}\gamma - \mathrm{s}\alpha\,\mathrm{s}\beta\,\mathrm{s}\gamma) + a(1-\mathrm{c}\alpha\,\mathrm{c}\gamma + \mathrm{s}\alpha\,\mathrm{s}\beta\,\mathrm{s}\gamma) \\ &+b\,\mathrm{s}\alpha\,\mathrm{c}\beta - c(\mathrm{s}\gamma\,\mathrm{c}\alpha + \mathrm{s}\alpha\,\mathrm{s}\beta\,\mathrm{c}\gamma) \end{aligned} \tag{2}$$

where, a, b and c represent the installation position of zero point of spot position measuring sensor 1 on the body. L is the distance between the sensors 1 and 2. H is the height difference between the two sensors. d_1 and d_2 are the measurement results of photoelectric sensor 1 and 2, β and γ are pitch angle and roll angle measured by inclinometer sensor.

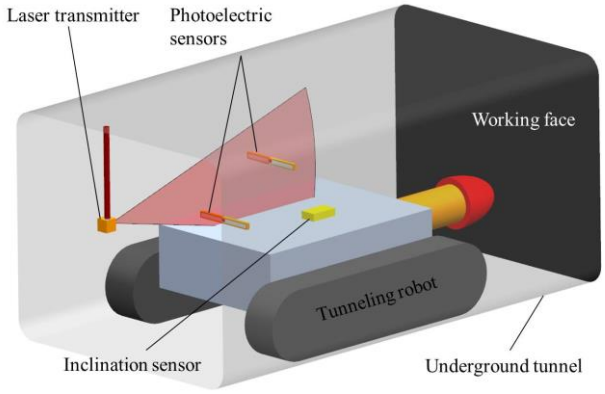

Fig.2 Pose detection system

4 Motion control method

4.1 Path planning

As mentioned earlier, the roadheader fuselage should be controlled to move smoothly without velocity jump due to its huge mass. At the same time, the error of the position and heading angle at the goal point should not exceed the allowable value. It seems that we should make a compromise between the positioning accuracy and movement smoothness. A control method based on deviation prediction model is proposed, the principle is as follows.

First, the deviation and heading angle of roadheader at the goal point are predicted, as shown in Fig. 3. Point P represents the geometric center of the roadheader. Point T represents the end point of the tunneling cycle. Point P_1 represents the predicted position as the roadheader moves along the initial direction without control input. e_0 represents the initial position error of the roadheader at the starting point, e_t represents the predicted position error of the roadheader at the end of the cycle as the current motion state is kept unchanged. α_0 represents the heading angle of the roadheader at the starting point. l is the forward distance of each excavation cycle.

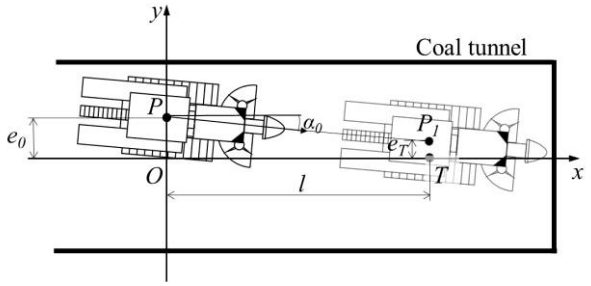

Fig.3 Principle of motion control method based on deviation prediction model

Then compare the predicted position error e_t with the initial position error e_0. If the position error trends to decrease, there is no need to change its current motion direction. So the path would be a straight line between the initial point P and predicted point P_1. In the other case, if the position error trends to increase, it is necessary to control the roadheader to move smoothly from the starting point P to the goal point T. In any case, the path which needs to be tracked will not be the tunnel middle line. The path planning in different cases is described mathematically as follows.

(1) $e_T < e_0$

The predicted position error e_T is less than the initial deviation e_0, so no control input is required in ideal situation. The roadheader needs walking along the initial direction as shown in Fig 4. The x-coordinate axis represents the middle line of the tunnel, the straight line with arrow represents the center line of the roadheader, and the dotted line represents the planned path. Therefore, the planning path is a straight line with starting point P and predicted point P_1. The function of planned path is

$$y = x\tan\alpha_0 + e_0, (0 \le x \le l) \tag{3}$$

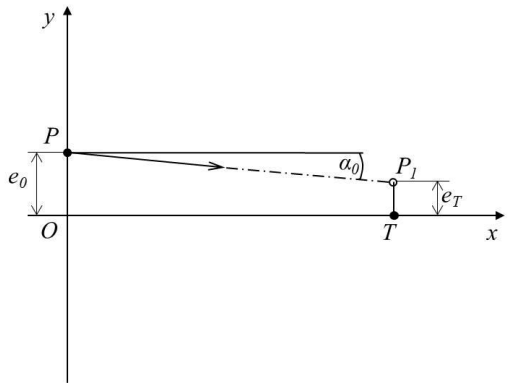

Fig.4 Path planning when $e_T < e_0$

(2) $e_T \ge e_0$

If the predicted position e_T is larger than the initial deviation e_0, the path should be re-planned. In Fig. 5, the dotted line denotes the planned path, a smooth curve joining starting point P and goal point T.

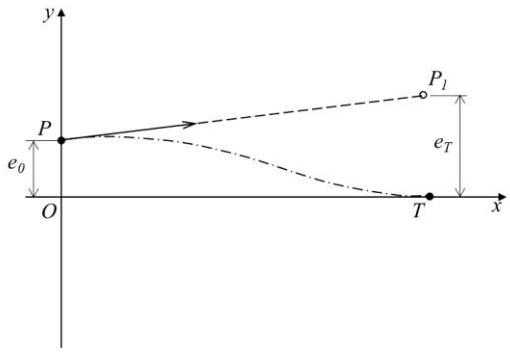

Fig.5 Path planning when when $e_T \ge e_0$

The path needs to meet two requirements. First, the adjustment to the movement of the roadheader should be reduced as much as possible. Second, the direction of the roadheader at goal point needs parallel to the tunnel middle line (i.e. the x-coordinate axis). To meet the above requirements, a cubic polynomial is used to fit the path which has the form

$$y = ax^3 + bx^2 + cx + d \tag{4}$$

where a, b, c and d is the coefficient of each term. The boundary conditions are as follows:

$$\begin{cases} y(0) = e_0 \\ y(l) = 0 \\ y'(0) = \tan\alpha_0 \\ y'(l) = 0 \end{cases} \tag{5}$$

Where, the first two equations represent the coordinates of roadheader at the starting point and goal point, respectively. The third equation means the initial direction of roadheader at starting point is tangent to the planned path. The forth equation means the x-coordinate axis is tangent to the planned path.

By substituting the boundary conditions (5) to equation (4), the coefficients are obtained

$$\begin{cases} a = \dfrac{l\tan\alpha_0 + 2e_0}{l^3} \\ b = -\dfrac{2l\tan\alpha_0 + 3e_0}{l^2} \\ c = \tan\alpha_0 \\ d = e_0 \end{cases} \tag{6}$$

where e_0 represents the initial position error of the roadheader at the starting point, α_0 represents the heading angle of the roadheader at the starting point. These two terms can be measured by pose detection system. l is the forward distance of each excavation cycle, which is determined by the requirement of tunneling process.

In addition, there is an extreme case needs to be

taken into account. If the initial position error is at extreme high level, it is considered to correct the deviation of the roadheader in multiple excavation cycles. Fig. 6 shows the principle of this strategy. Note that the ultimate goal of motion control is to ensure the accuracy of tunnel direction and the tunnel section and make both sides of the tunnel as smooth as possible. This means that the position difference between the starting point and the goal point in a driving cycle should not be too large. Therefore, when the initial position error is too large, it may be necessary to gradually correct the lateral displacement deviation in multiple driving cycles.

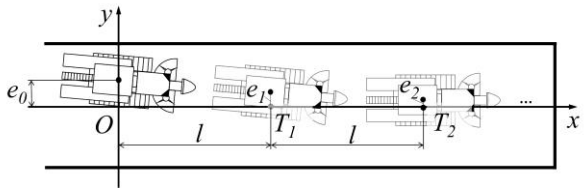

Fig. 6 The control strategy in multiple excavation cycles

It is possible to set a maximum adjustment [*e*] for each excavation cycle. If initial position error e_0 is larger than [*e*], point *T'* will be set as the goal point as shown in Fig. 7. In this way, the *y* coordinate of the transition goal point *T'* has the form

$$y_{T'} = e_0 - [e] \tag{7}$$

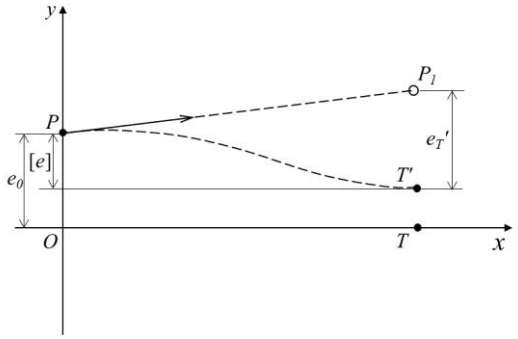

Fig.7 Planning path when in first excavation cycle

In this case, the boundary conditions are as follows:

$$\begin{cases} y(0) = e_0 \\ y(l) = y_{T'} \\ y'(0) = \tan\alpha_0 \\ y'(l) = 0 \end{cases} \tag{8}$$

By substituting the boundary conditions (8) to equation (4), the coefficients are obtained

$$\begin{cases} a = \dfrac{l\tan\alpha + 2(e_0 - y_{T'})}{l^3} \\ b = -\dfrac{2l\tan\alpha_0 + 3(e_0 - y_{T'})}{l^2} \\ c = \tan\alpha_0 \\ d = e_0 \end{cases} \tag{9}$$

4.2 Trajectory tracking

Firstly, the kinematics model of the roadheader is built as shown in Fig. 8.

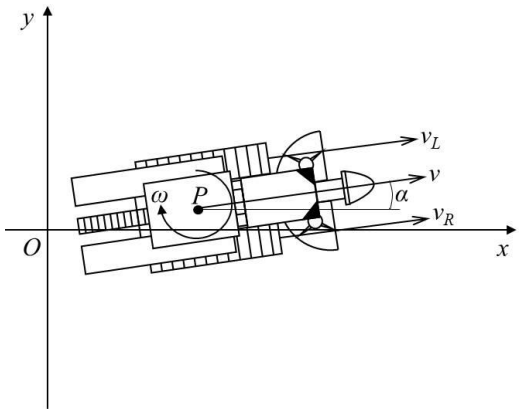

Fig. 8. Kinematic model of roadheader fuselage

Where, the coordinate system *Oxy* is the global coordinate system. The *x*-axis is the middle line of the tunnel, the *y*-axis is perpendicular to the *x*-axis on the plane of tunnel floor. The origin *O* is the initial position of each excavation cycle. *P* is the center of the roadheader fuselage, with the coordinate pair (*x*, *y*) in the global coordinate system. *v* is the velocity of the fuselage in the global coordinate system. v_L and v_R is the linear velocity of left track and right track, respectively. α is the heading angle of the fuselage, ω is angular velocity of the fuselage. *B* is the width of the fuselage, that is, the distance between the left and right tracks.

It is easy to get the kinematics model of the fuselage

$$\begin{bmatrix} \dot{x} \\ \dot{y} \\ \dot{\alpha} \end{bmatrix} = \begin{bmatrix} \cos\alpha & 0 \\ \sin\alpha & 0 \\ 0 & 1 \end{bmatrix} \begin{bmatrix} v \\ \omega \end{bmatrix} \tag{10}$$

Since the angular velocity of each point on the fuselage is equal, we get

$$\begin{pmatrix} v_L \\ v_R \end{pmatrix} = v + \begin{pmatrix} B/2 \\ -B/2 \end{pmatrix} \omega \tag{11}$$

Convert the trajectory tracking error to fuselage coordinate system

$$\begin{pmatrix} e_x \\ e_y \\ e_\alpha \end{pmatrix} = \begin{pmatrix} \cos\alpha & \sin\alpha & 0 \\ -\sin\alpha & \cos\alpha & 0 \\ 0 & 0 & 1 \end{pmatrix} \begin{pmatrix} x_r - x \\ y_r - y \\ \alpha_r - \alpha \end{pmatrix} \tag{12}$$

where, e_x, e_y and e_α are the trajectory tracking errors. x_r, y_r and α_r are the expected pose and position on the reference path. x, y and α are the real pose and position.

The dynamic error model of trajectory tracking has the form (Bian et al. 2018)

$$\begin{pmatrix} \dot{e}_x \\ \dot{e}_y \\ \dot{e}_\alpha \end{pmatrix} = \begin{pmatrix} -1 \\ 0 \\ 0 \end{pmatrix} v_r + \begin{pmatrix} e_y \\ -e_x \\ -1 \end{pmatrix} \omega_r + \begin{pmatrix} v\cos e_\alpha \\ v\sin e_\alpha \\ \omega \end{pmatrix} \tag{13}$$

where, $\dot{e}_x$, $\dot{e}_y$ and $\dot{e}_\alpha$ are the velocity deviations of $\dot{x}$, $\dot{y}$ and $\dot{\alpha}$ relative to the expected values respectively. v_r is the expected velocity of fuselage and ω_r is the expected angular velocity. Trajectory tracking is the process of finding a suitable controller (i.e. control law) to make the tracking errors tend to zero. We used the controller based on Lyapunov stability theory proposed in reference (Giuseppe et al. 2002).

$$\begin{pmatrix} v \\ \omega \end{pmatrix} = \begin{pmatrix} v_r \cos e_\alpha + k_1 e_x \\ \omega_r + \dfrac{k_2 v_r e_y \sin e_\alpha}{e_\alpha} + k_3 e_\alpha \end{pmatrix} \tag{14}$$

where k_1, k_2 and k_3 are the control gains (Alessandro et al. 2001) with functions

$$\begin{pmatrix} k_1 \\ k_2 \\ k_3 \end{pmatrix} = \begin{pmatrix} 2\varsigma\sqrt{\omega_r^2 + g v_r^2} \\ g \\ 2\varsigma\sqrt{\omega_r^2 + g v_r^2} \end{pmatrix} \tag{15}$$

where g and ζ (Canudas et al. 1993) are positive real numbers of a fixed pole placement strategy.

5 Simulation experiments and discussion

5.1 Experiment setup

To verify the performance of the motion control method, the trajectory tracking simulation experiments are carried. In the experiments, the parameters including position, heading angle, velocity and angular velocity can be measured or calculated. The control outputs are the actual velocity and angular velocity of the roadheader. Fig. 9 illustrates the control model.

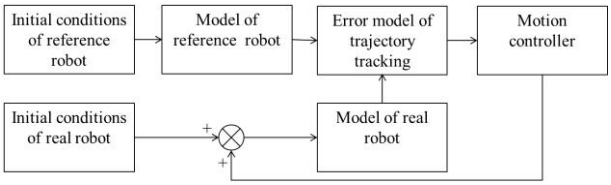

Fig. 9 Block diagram of trajectory tracking control model

The initial conditions reference fuselage contains the initial position, heading angle, velocity and angular velocity. The model of reference fuselage or real fuselage calculates the trajectory to time according to the input velocity and angular velocity. The trajectory tracking error model calculates the trajectory tracking error and the motion controller calculates the velocity and angular velocity for control input according the control law and tracking error.

5.2 Simulation results and discussion

5.2.1 Tracking of straight line

For the case mentioned in Fig. 4, the planned path is a straight line with equation (3) rather the x-coordinate which represents the tunnel middle line. The setting is as follows: the initial position error is assumed to be e_0=0.04 m, initial heading angle is α_0= - 2°, the velocity of fuselage is 0.1 m/s, the forward distance is l=1 m. The distance between left and right track is B=2.3 m, and the radius of driving wheel is R=0.3 m. The coefficients g and ζ are set to 50 and 0.9, respectively. Fig. 10-15 compare the kinematic characteristics with and without path planning, including trajectory curve, velocity and angular velocity of fuselage, angular acceleration of left and right driving wheels.

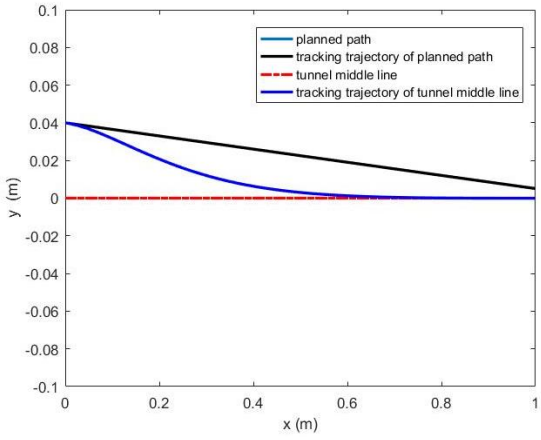

Fig. 10 Tracking trajectory of different target paths

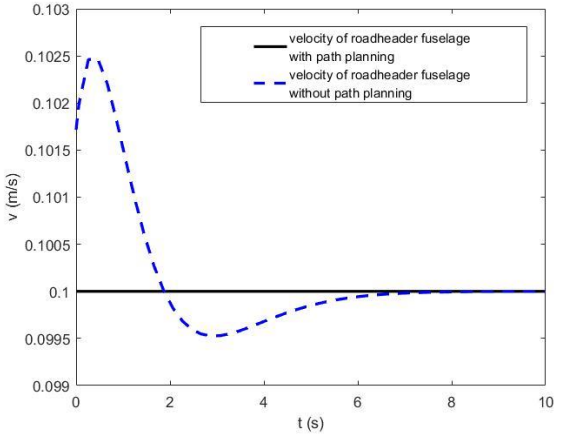

Fig. 11 Velocity of roadheader fuselage

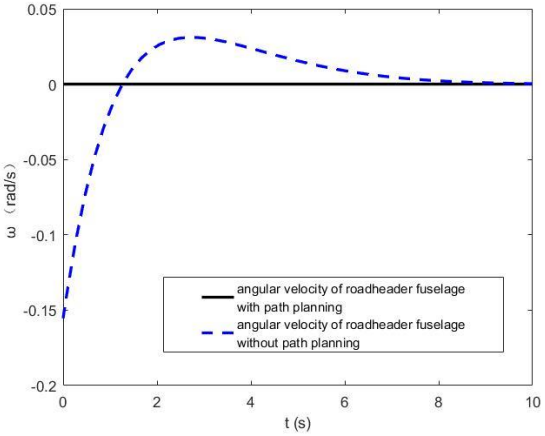

Fig. 12 Angular velocity of roadheader fuselage

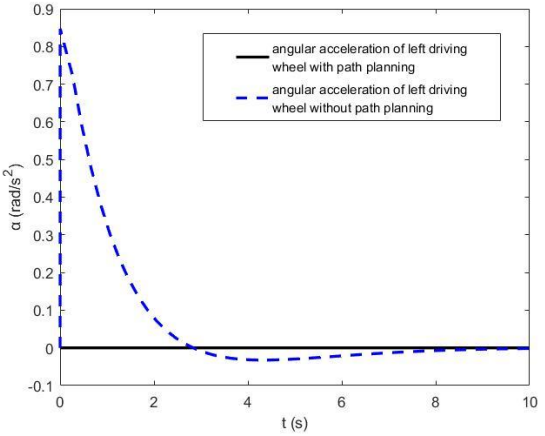

Fig. 13 Angular acceleration of left driving wheel

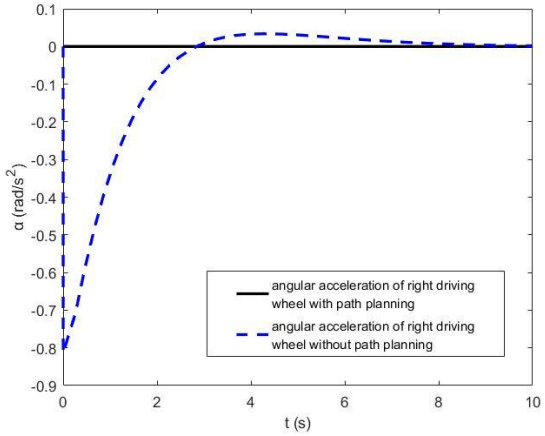

Fig. 14 Angular acceleration of right driving wheel

The findings are as follows:

(1) When the target path is the planned path, the tracking trajectory coincides with the planned path, the velocity of roadheader fuselage is constant, the angular velocity of roadheader fuselage and accelerations of both driving wheels are always zero.

(2) When the target path is the tunnel middle line, the velocity of the fuselage has a slight fluctuation at initial stage, the angular velocity at initial point reaches 0.15 rad/s and gradually decreases to zero. The worst part is that the maximum accelerations of both driving wheels are about 0.8 rad/s^2 at the starting point, which are far larger than that of the planned path.

It is concluded that in this case, the proposed motion method performs well than that without path planning in terms of motion smoothness, although the position error of the proposed method is slightly larger than that of the conventional method.

5.2.1 Tracking of polynomial curve

For the case mentioned in Fig. 5, the planned path is a cubic polynomial with equation (4) rather the x-coordinate which represents the middle line of the tunnel. The setting is as follows: the initial position error is assumed to be e_0=0.04 m, initial heading angle is α_0=2°, the remaining initial conditions are the same as previously described. Fig. 15- 19 show the kinematic characteristics of the roadheader of different target paths.

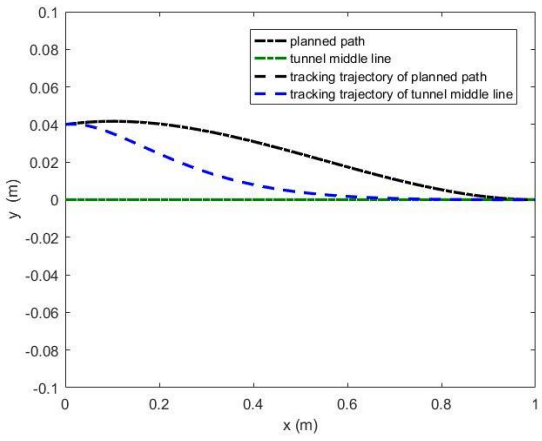

Fig. 15 Tracking trajectory of different target paths

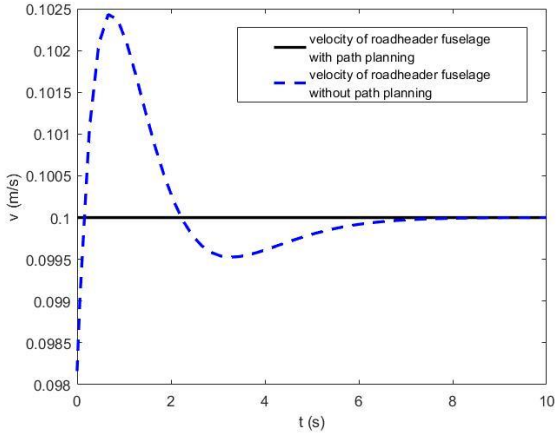

Fig. 16 Velocity of roadheader fuselage

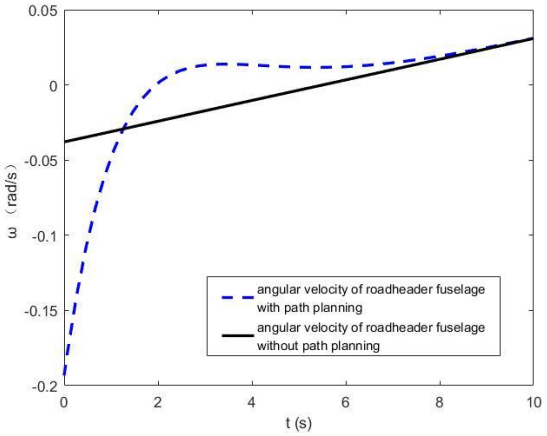

Fig. 17 Angular velocity of roadheader fuselage

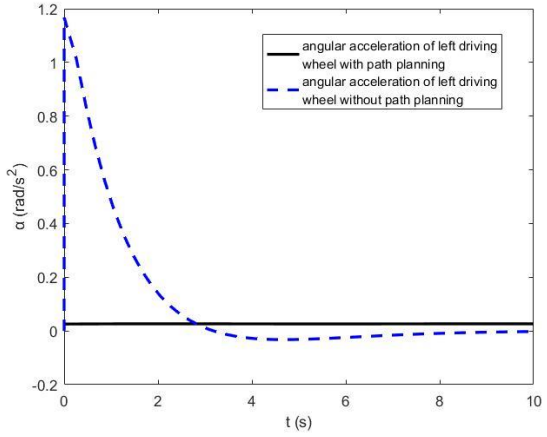

Fig. 18 Angular acceleration of left driving wheel

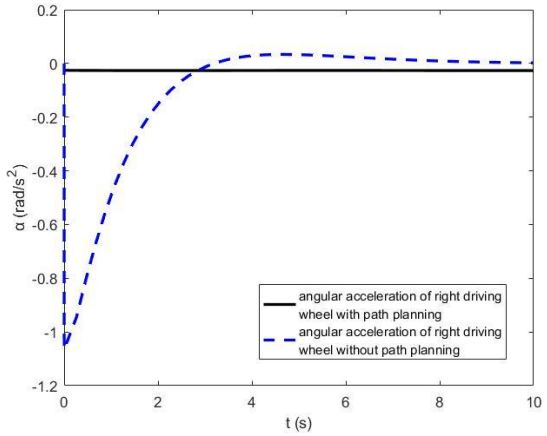

Fig. 19 Angular acceleration of right driving wheel

The findings are as follows:

(1) When the target path is the planned path, the tracking trajectory seems smoother than which tracks the tunnel middle line. the velocity of roadheader fuselage barely changes, the angular velocity of roadheader fuselage changes linearly, the angular velocity of roadheader fuselage and accelerations of both driving wheels has little change at 0.027 rad/s^2.

(2) When the target path is the tunnel middle line, the velocity of the fuselage has a slight fluctuation at initial stage as well, the angular velocity at initial point reaches 0.2 rad/s and gradually decreases to zero. Similarly, the accelerations of both driving wheels at the starting point are high, about 44 times to that with path planning.

To estimate the amount of control input, a performance index called control effort is defined. The control effort is scored as the absolute value of the curvature increments for all the control intervals (Jes u´s M 2009). Table 1 show the comparison of the control effort with and without path planning. It is easy to find that the control effort is smaller when the path planning link is added.

Table 1 Control effort under different conditions

Initial condition	With path planning	Without path planning
e_0=0.04mm, α_0=-2°	0	0.0380
e_0=0.04mm, α_0= 2°	0.0160	0.0529

From the above results, the proposed motion control method is with stable control process and less control effort. Compared with the method of tracking the tunnel middle line, the proposed method is more appropriate for the motion control of roadheader fuselage.

6 Conclusion

The motion control method of roadheader fuselage is proposed in this paper, which plans the path for tracking based on the predicted position of goal point. Then a trajectory tracking method based on Lyapunov stability theory is used to track the planned path. To verify the performance of the proposed motion control

method, simulation experiments were carried out. Experiment results shows that on different initial conditions, the proposed control method is with low control effort and high stability. It is especially adapted for the motion control of roadheader fuselage with huge mass.

References

Wang GF, Zhao GR, Ren HW (2019) Analysis on key technologies of intelligent coal mine and intelligent mining. Journal of China Coal Society 44(1):.34-41.https://doi.org/10.13225./.j.cnki.jccs.2018.5034

Wang GF, Wang H, Ren HW, Zhao GR, Pang YH, Du YB, Zhang JH, Hou G (2018) 2025 scenarios and development path of intelligent coal mine. Journal of China Coal Society 43(2): 295-305. https://doi.org/ 10.13225 / j.cnki.jccs.2018.0152

Wang YJ, Zhang JG, Ma Z (2015) Research status and development tendency of mine fully-mechanized heading equipment technology. Coal science and technology 43(11): 87-90+21.

Tian Y (2019) Inertial navigation positioning method of roadheader based on zero-velocity update. Industry and Mine Automation 45(8): 70-73.

Tao YF, Zong K, Zhang MJ, Jia WH, Fu SC, Yang JJ, Wu M (2015) A position and orientation measurement method of single-station, multipoint and time-sharing for roadheader body based on iGPS. Journal of China Coal Society 40(11): 2611-2616. https://doi.org/ 10.13225 / j.cnki.jccs.2015.7063

Zhao XL (2011) Research of identification of coal and rock and load torque observer of roadheader based on multi-sensor information fusion, Ph.D. dissertation. China University of Mining and Technology, Beijing, China.

Fu SC, Li YM, Yang JJ, Jia WH, Tao YF, Zong K, Zhang MJ, Wu M (2015) Research on autonomous positioning and orientation method of roadheader based on Ultra Wide-Band technology. Journal of China Coal Society 40(11): 2603-2610.https://doi.org/10.13225/j.cnki.jccs.2015.7064

Li R (2012) Research on an Automatic Detection System for the Position and Orientation Parameters of Boom-type Roadheader Body, Ph.D. dissertation, Dept. China University of Mining and Technology.

Moshayedi A J, Roy A S, Liao L (2019) PID Tuning Method on AGV (automated guided vehicle) Industrial Robot. Journal of Simulation & Analysis of Novel Technologies in Mechanical Engineering 12(4):0053-0066.

Coulter R C (1992) Implementation of the Pure Pursuit Path Tracking Algorithm. Carnegie Mellon.

Jesu´s Morales, Jorge L, Martı´nez, Marı´a A, Martı´nez, Anthony Mandow (2009) Pure-Pursuit Reactive Path Tracking for Nonholonomic Mobile Robots with a 2D Laser Scanner. Eurasip Journal on Advances in Signal Processing. https://doi.org/10.1155/2009/935237

Hu JM, Hu YH, Chen HY, Liu K (2019) Research on Trajectory Tracking of Unmanned Tracked Vehicles Based on Model Predictive Control. ACTA ARMAMENTARII 40(3).

Skakauskas P , Grakovski A (2021) Efficiency Analysis of Stanley's Controller Applied to the Autonomous Ground Vehicle Movement Control Under Effect of Various Perturbations.

Zhang XH, Zhao JX, Yang WJ, Zhang C (2021) Vision-based Navigation and Directional Heading Control Technologies of Boom-type Roadheader. Journal of China Coal Society. https://doi.org/ 10.13225/j.cnki.jccs.ZN20.0357

Bian YM, Yang M, Liu YC, Yang G (2018) Research on trajectory tracking control of a tracked mobile robot. Chinese journal of construction machinery 16(3): 189-193.

Giuseppe Oriolo, Alessandro De Luca, Marilena Vendittelli (2002) WMR Control Via Dynamic Feedback Linearization: Design, Implementation, and Experimental Validation. IEEE Transactions on Control Systems Technology 10(6): 835-852.

Alessandro De Luca, Giuseppe Oriolo, and Marilena

Vendittelli (2001) Control of Wheeled Mobile Robots: An Experimental Overview. RAMSETE-Articulated and Mobile Robotics for Services and Technologies. 181-226.

C. Canudas de Wit, H. Khennouf, C. Samson, O. J. Sørdalen (1993) Non-linear control design for mobile robots. World Scientific 11:131-156.

Competing interests

The authors declare that they have no known competing financial interests or personal relationships that could have appeared to influence the work reported in this paper.

Funding

This work was supported in part by the National Natural Science Foundation of China (51874157), in part by the National Key Research and Development Project of China (2017YFC0804305), in part by the Natural Science Foundation of Liaoning Province of China (2019-M-161).

Authors' contributions

Hongyue Chen: Conceptualization, Methodology

Wei Yang: Writing - Original Draft, Data curation

Desheng Zhang: Writing- Reviewing & Editing, Validation

Song Xiao: Software

Acknowledgments

This work was supported in part by the National Natural Science Foundation of China (51874157), in part by the National Key Research and Development Project of China (2017YFC0804305), in part by the Natural Science Foundation of Liaoning Province of China (2019-M-161).

Author information

Hongyue Chen received the B.S. degree from the Liaoning Technical University, Fuxin, China, in 2005, the M.S. degree from the Liaoning Technical University in 2008, and the Ph.D. degree in Liaoning Technical University in 2012. He is currently a Professor and Ph.D. Supervisor with the Liaoning Technical University. His research interests includes coal mine machinery design, coal mine machinery navigation and mining machinery automatization.

Wei Yang received the B.S. and M.S.degrees in mechanical engineering from the Jilin University, Jilin, China, in 2005 and 2007, respectively. He is currently pursuing the Ph.D. degree in mechanical engineering in Liaoning Technical University. His research interests include vehicle guidance, mining machinery design and vision-based position measurement.

Desheng Zhang received the B.S. degree from the China University of Mining and Technology, Beijing , China, in 2006, the M.S. degree from the China University of Mining and Technology in 2008, and the Ph.D. degree in China University of Mining and Technology in 2011. His research interest is coal mine machinery design.

Song Xiao is currently working in Shaanxi Yanchang Petroleum Balasu Coal Industry Co., Ltd. His research interest is coal mine machinery design.

Figures

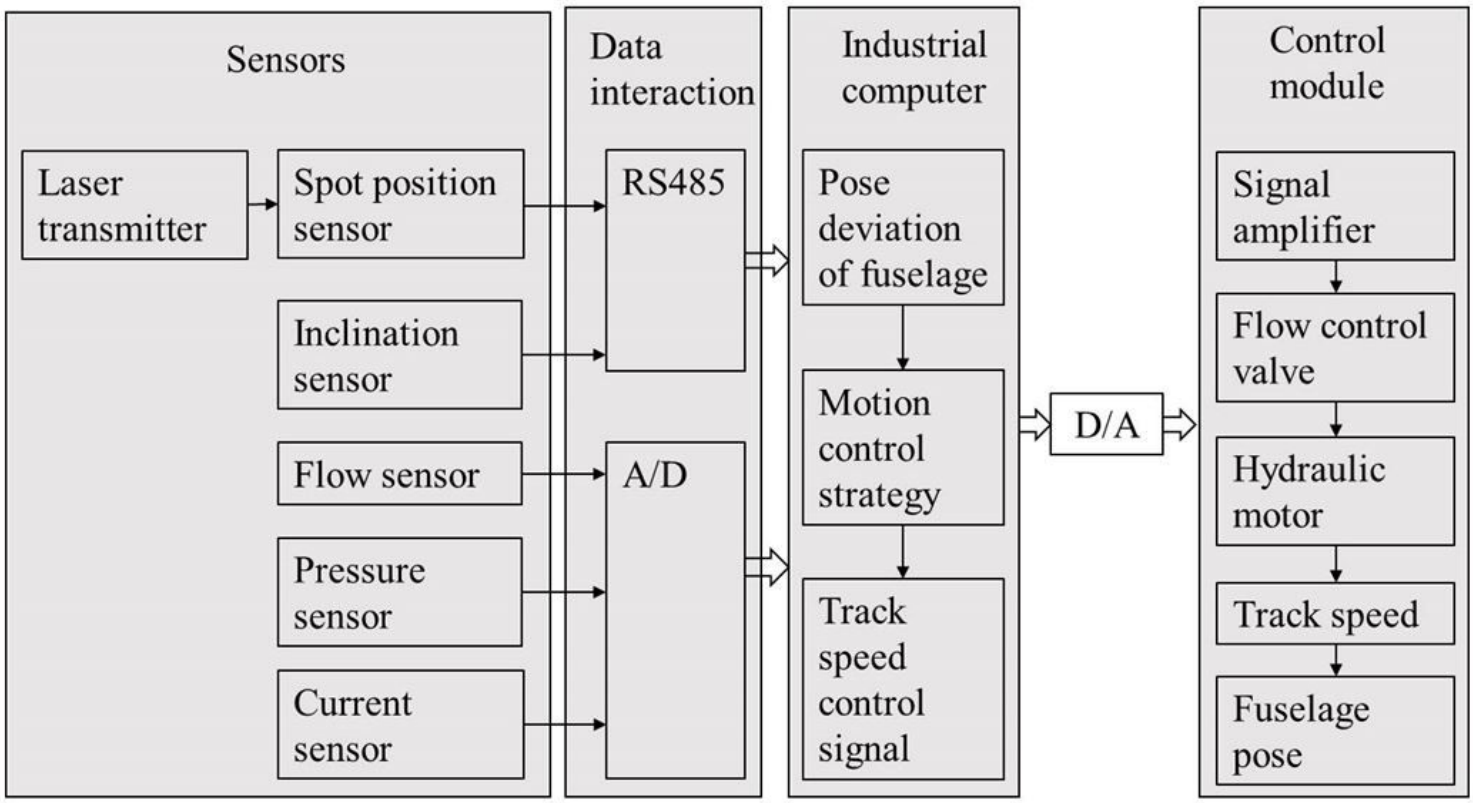

Figure 1

Overall design of motion control system

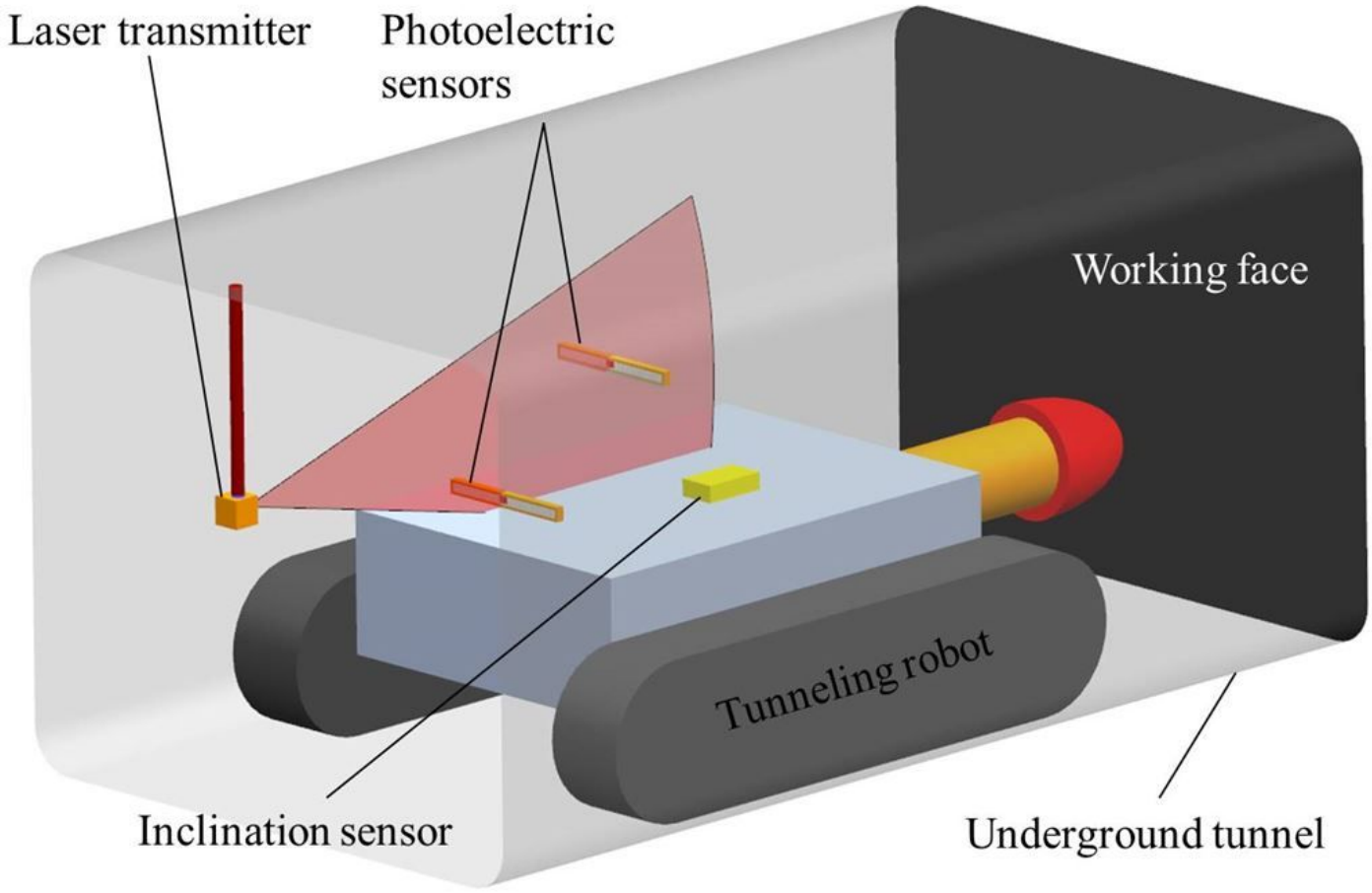

Figure 2

Pose detection system

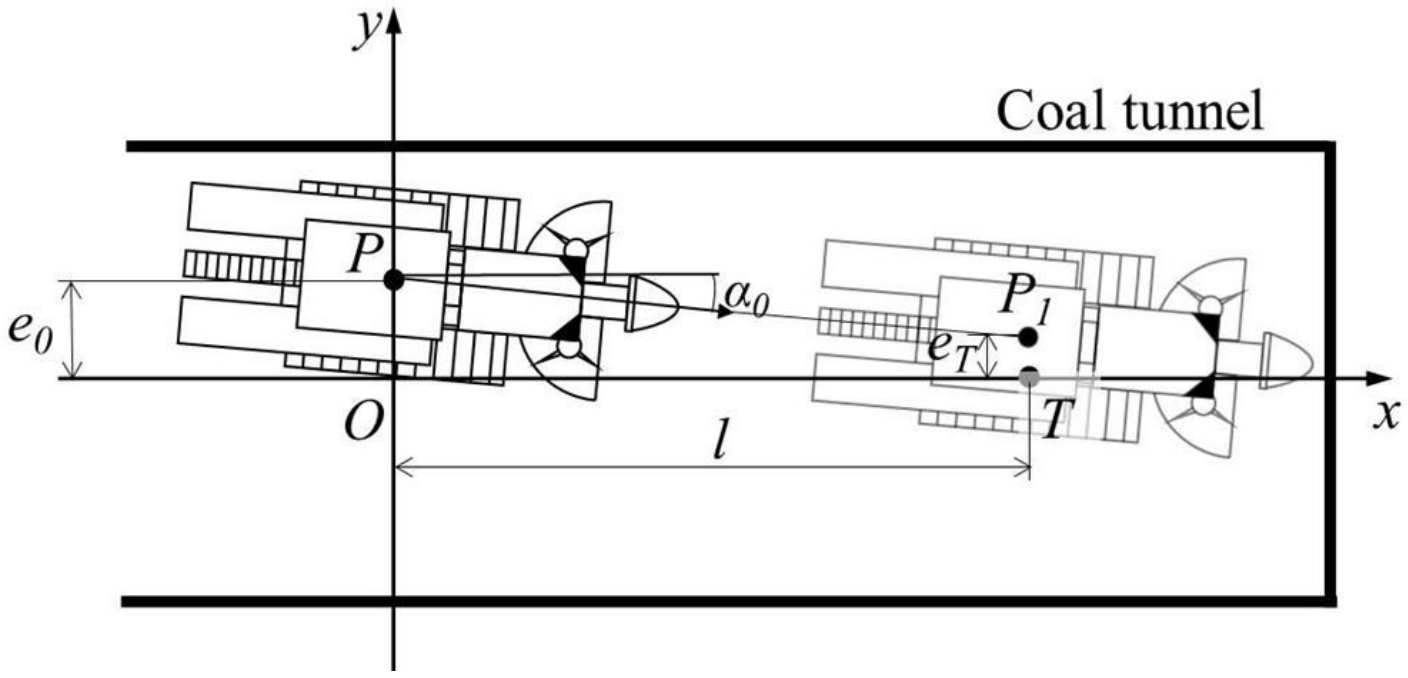

Figure 3

Principle of motion control method based on deviation prediction model

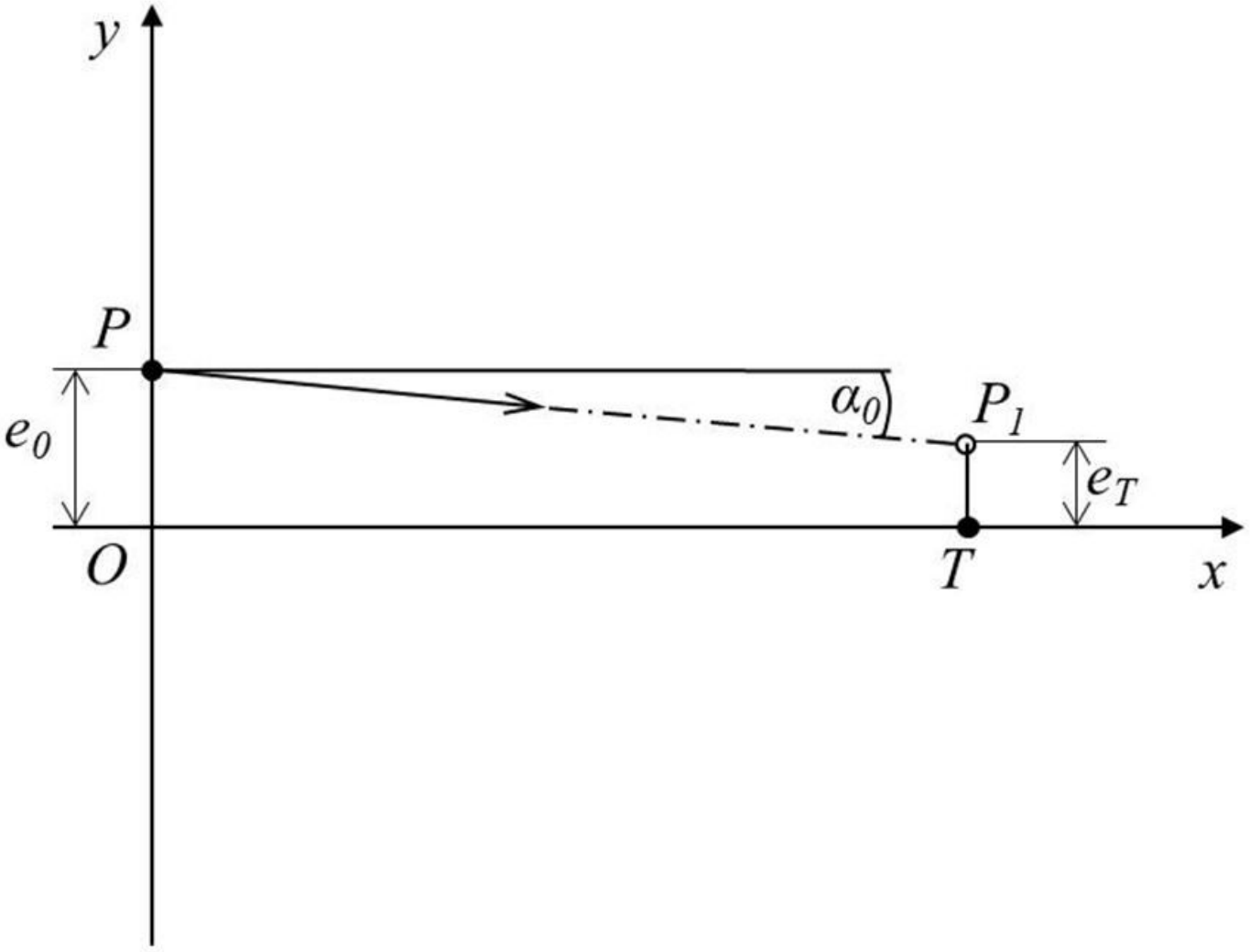

Figure 4

Path planning when eT<e0

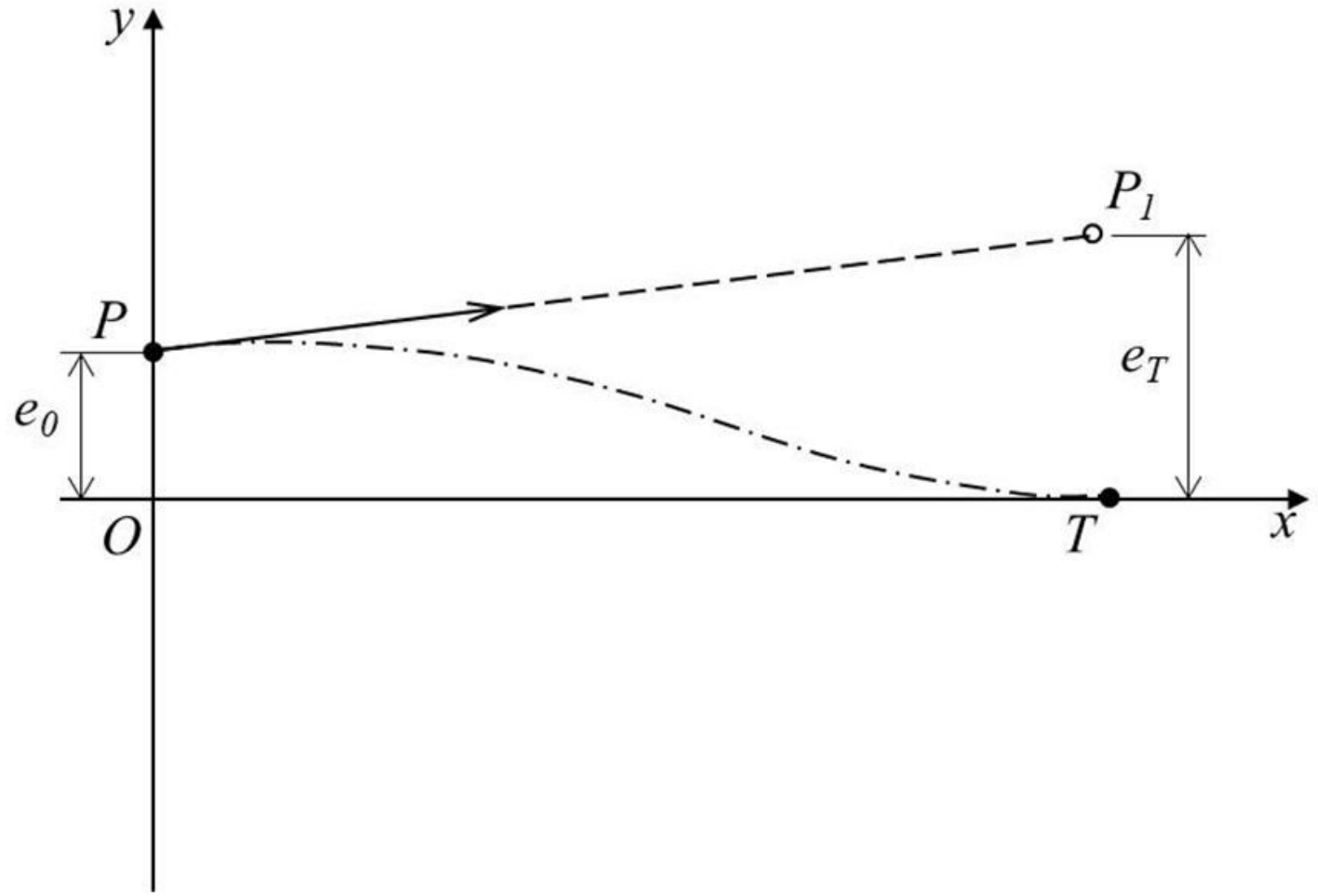

Figure 5

Path planning when when eT≥e0

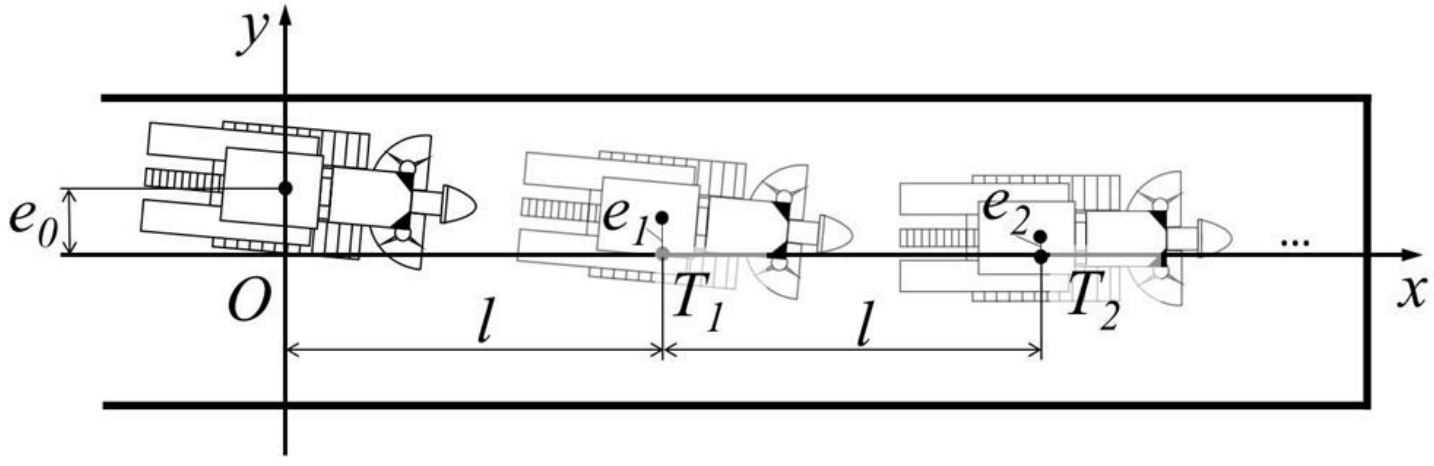

Figure 6

The control strategy in multiple excavation cycles

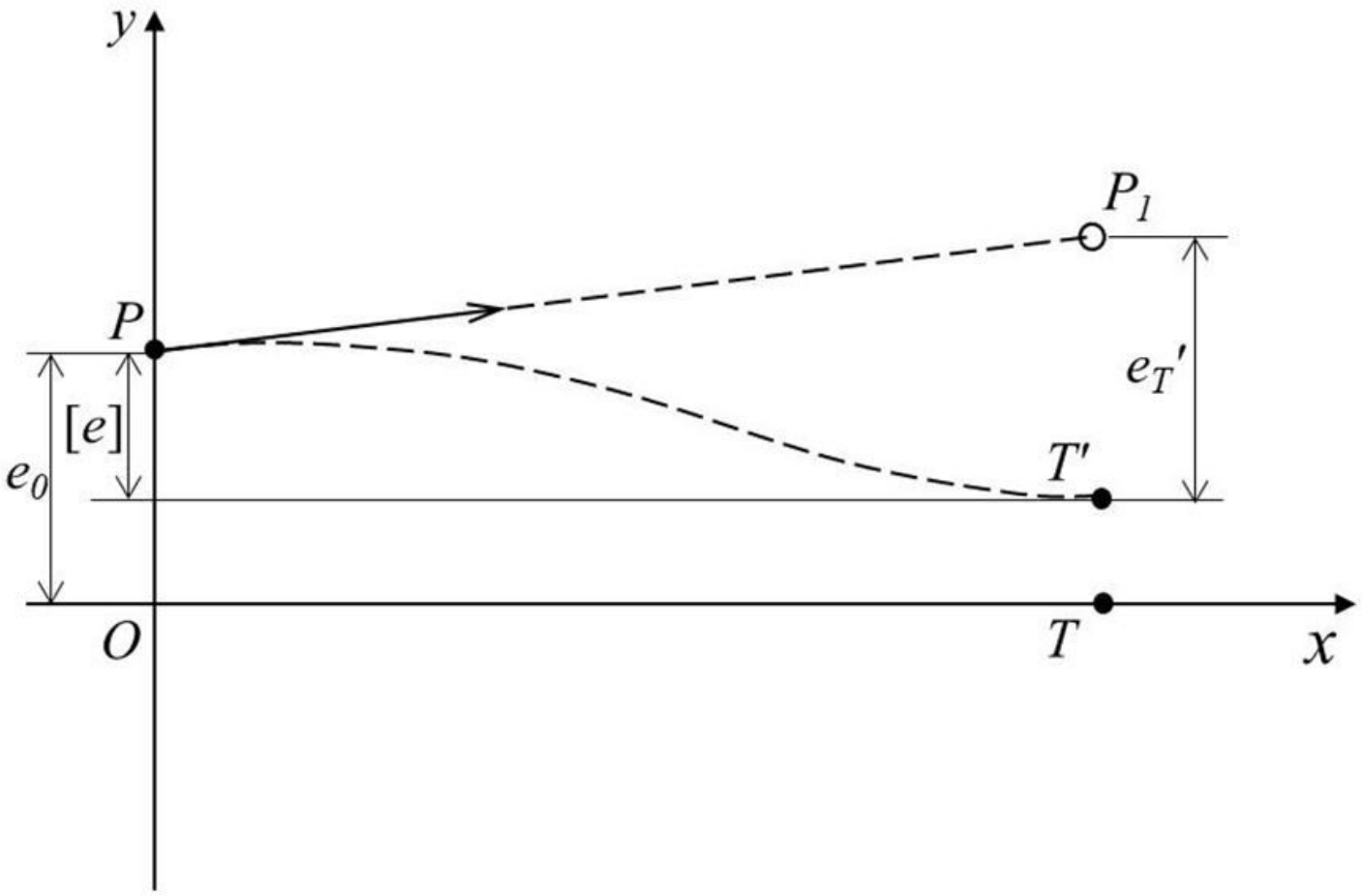

Figure 7

Planning path when in first excavation cycle

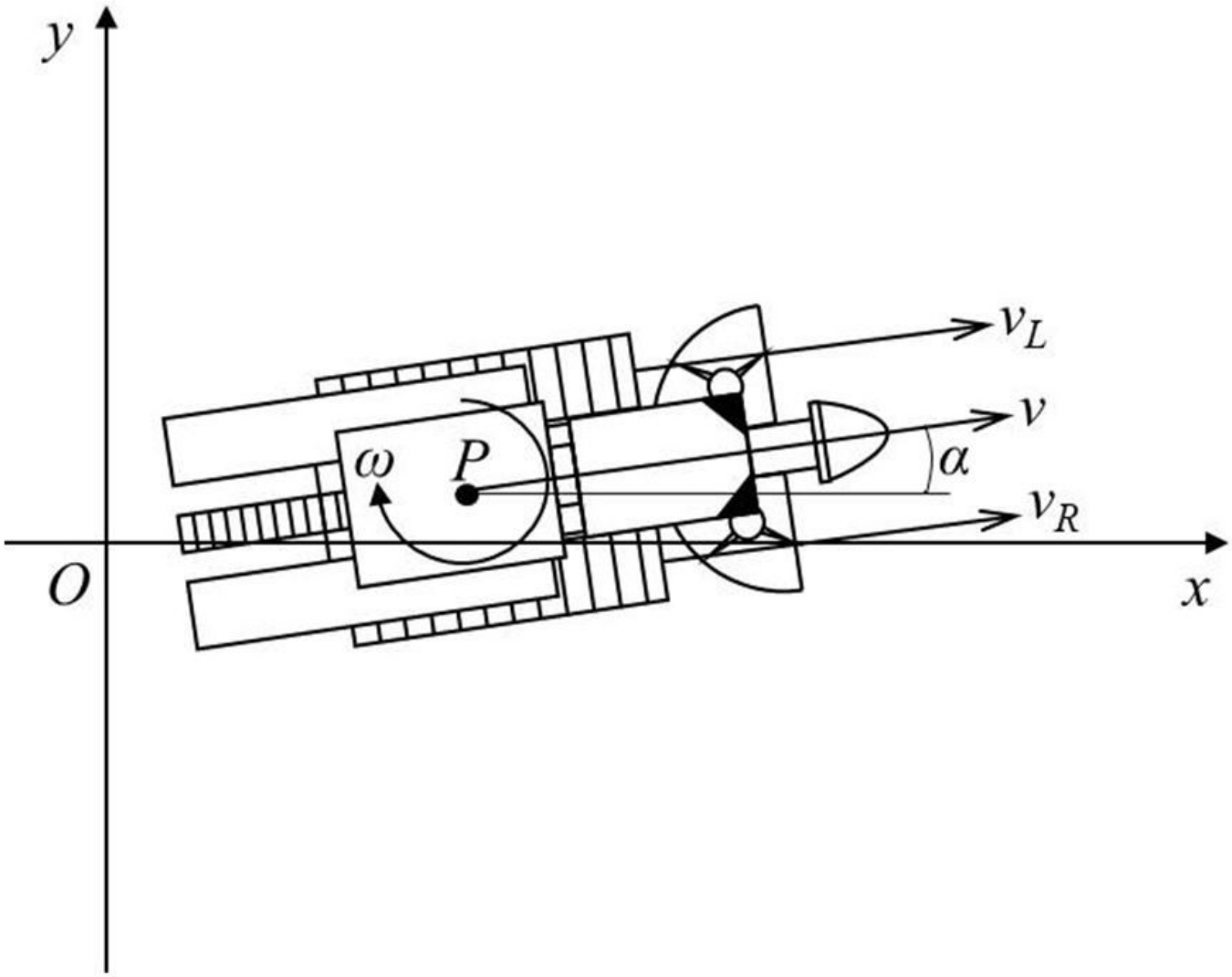

Figure 8

Kinematic model of roadheader fuselage

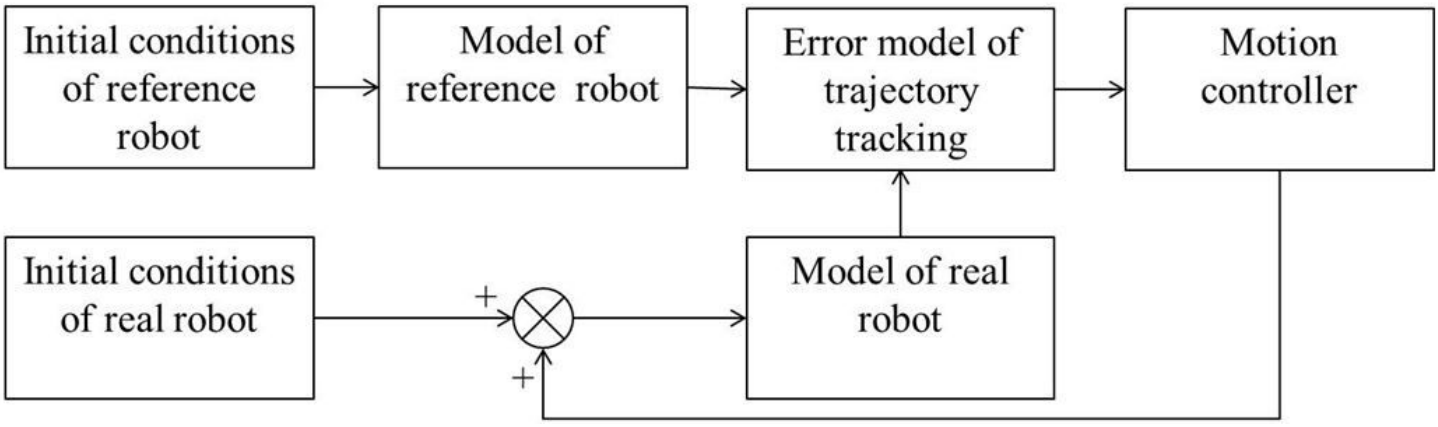

Figure 9

Block diagram of trajectory tracking control model

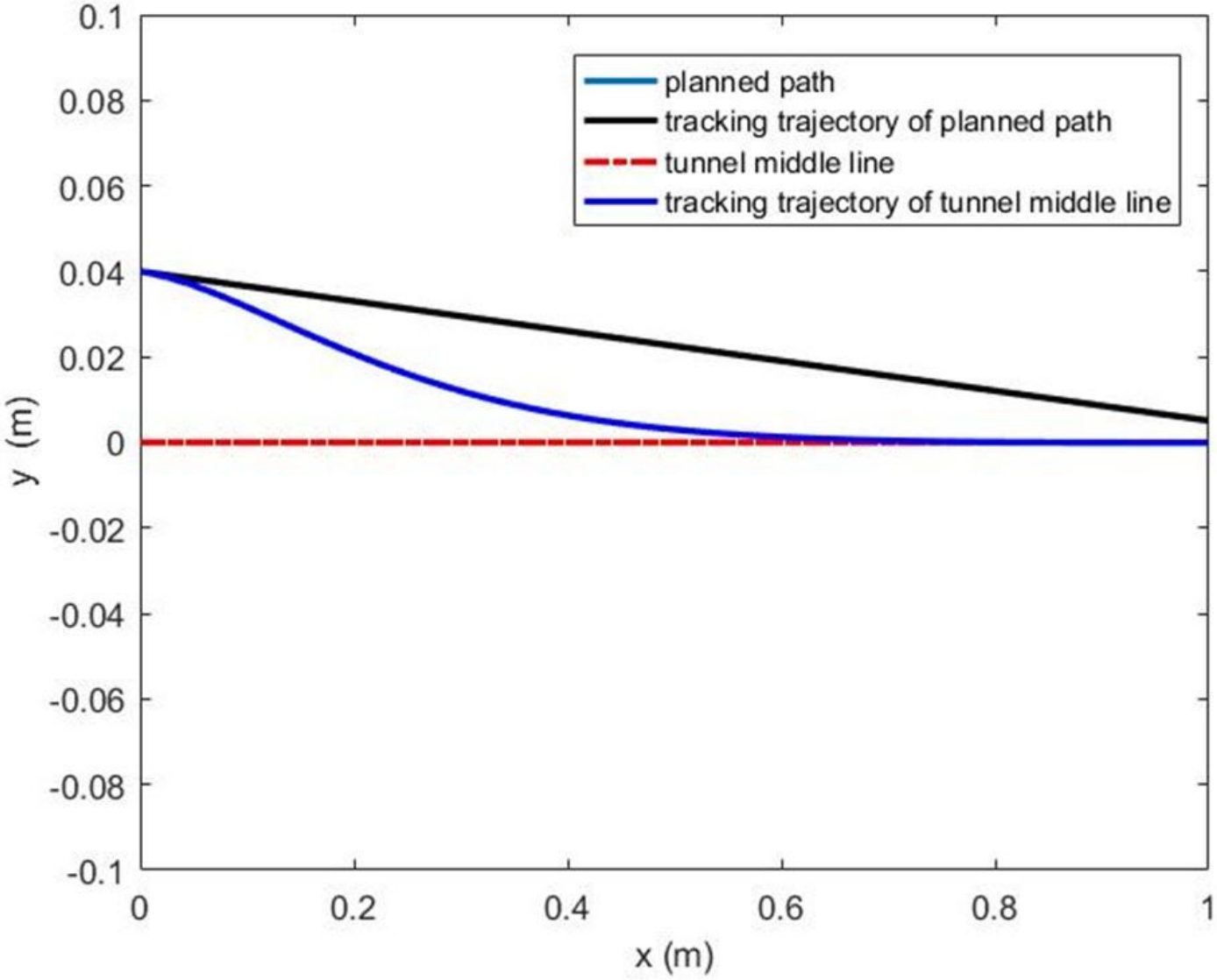

Figure 10

Tracking trajectory of different target paths

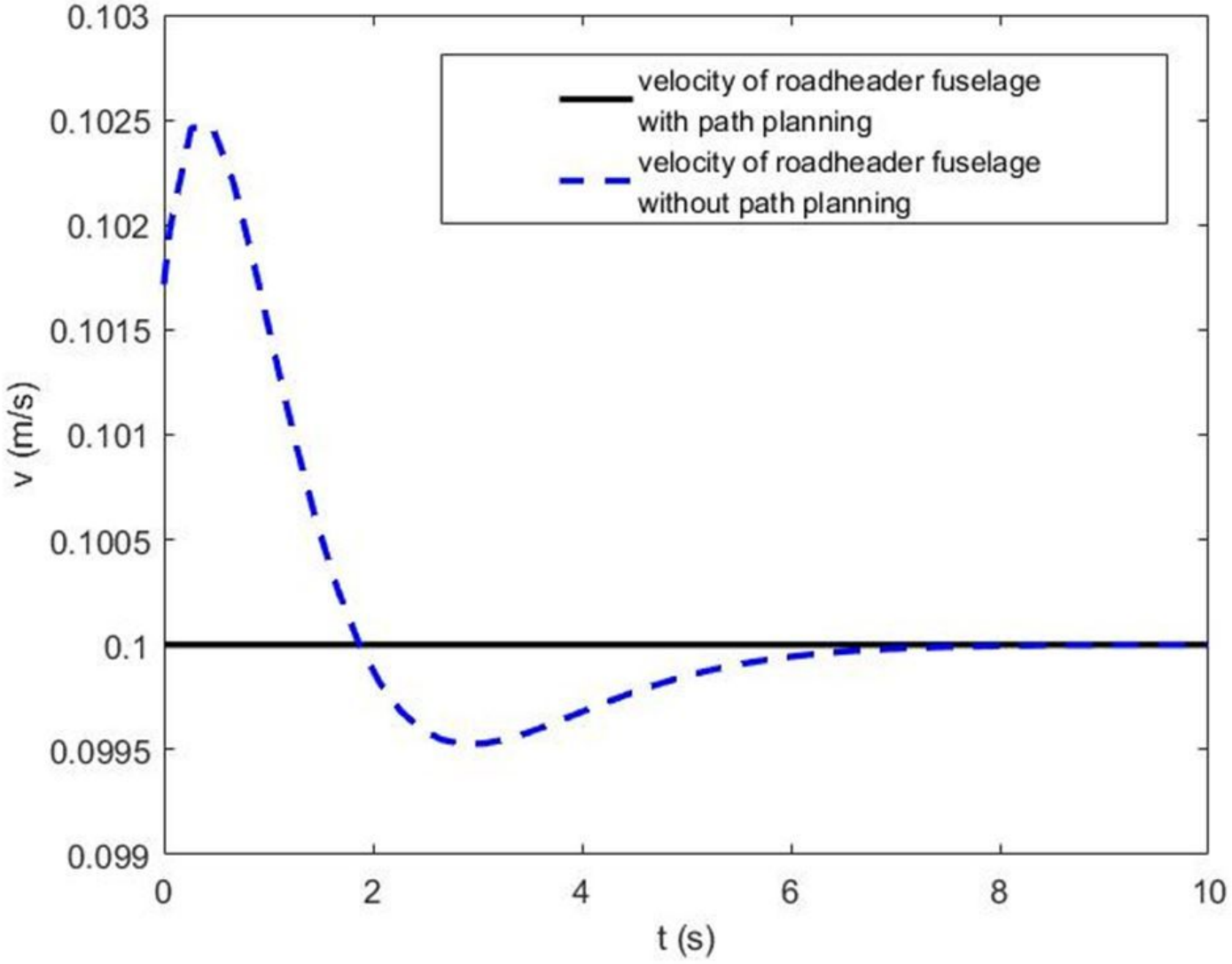

Figure 11

Velocity of roadheader fuselage

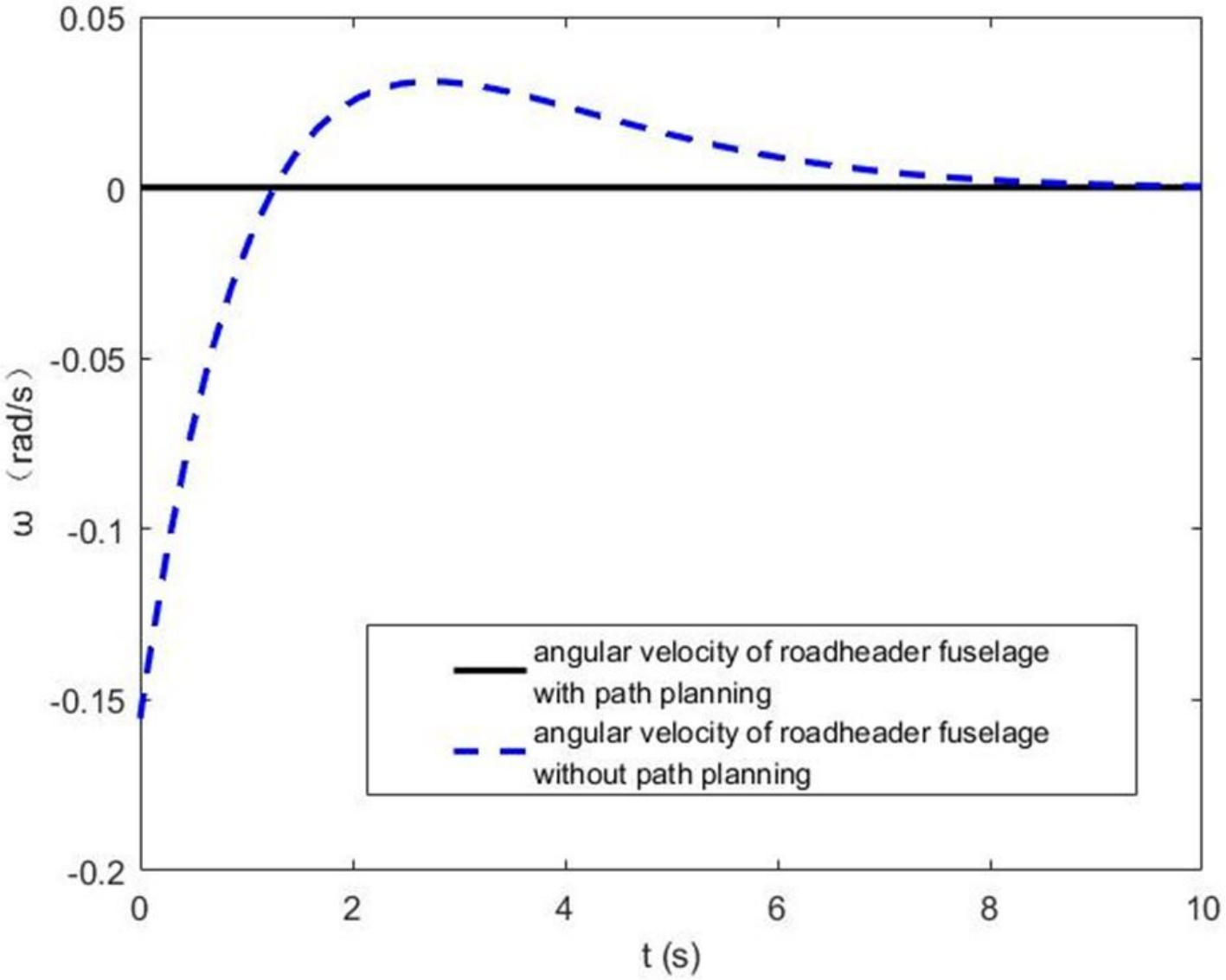

Figure 12

Angular velocity of roadheader fuselage

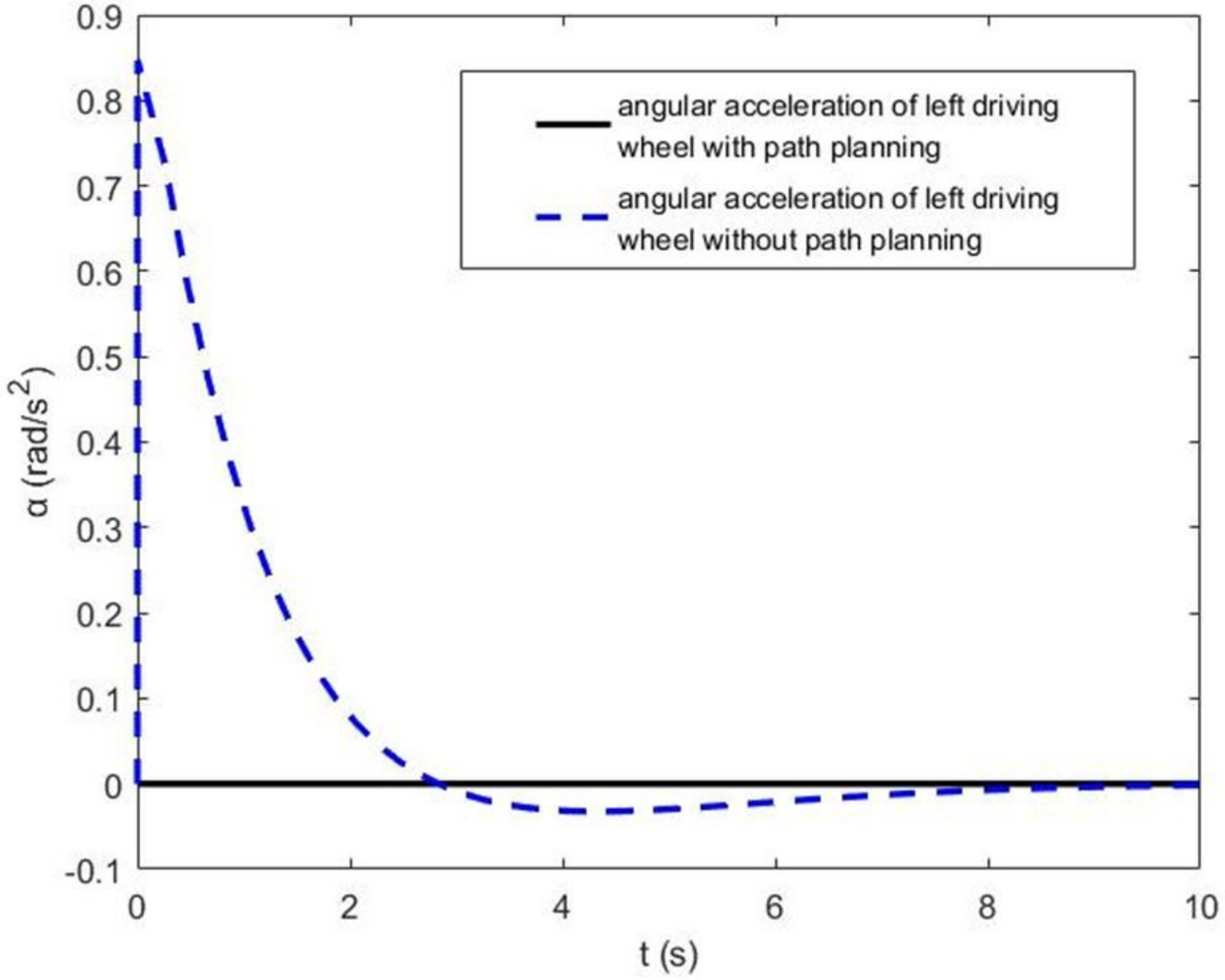

Figure 13

Angular acceleration of left driving wheel

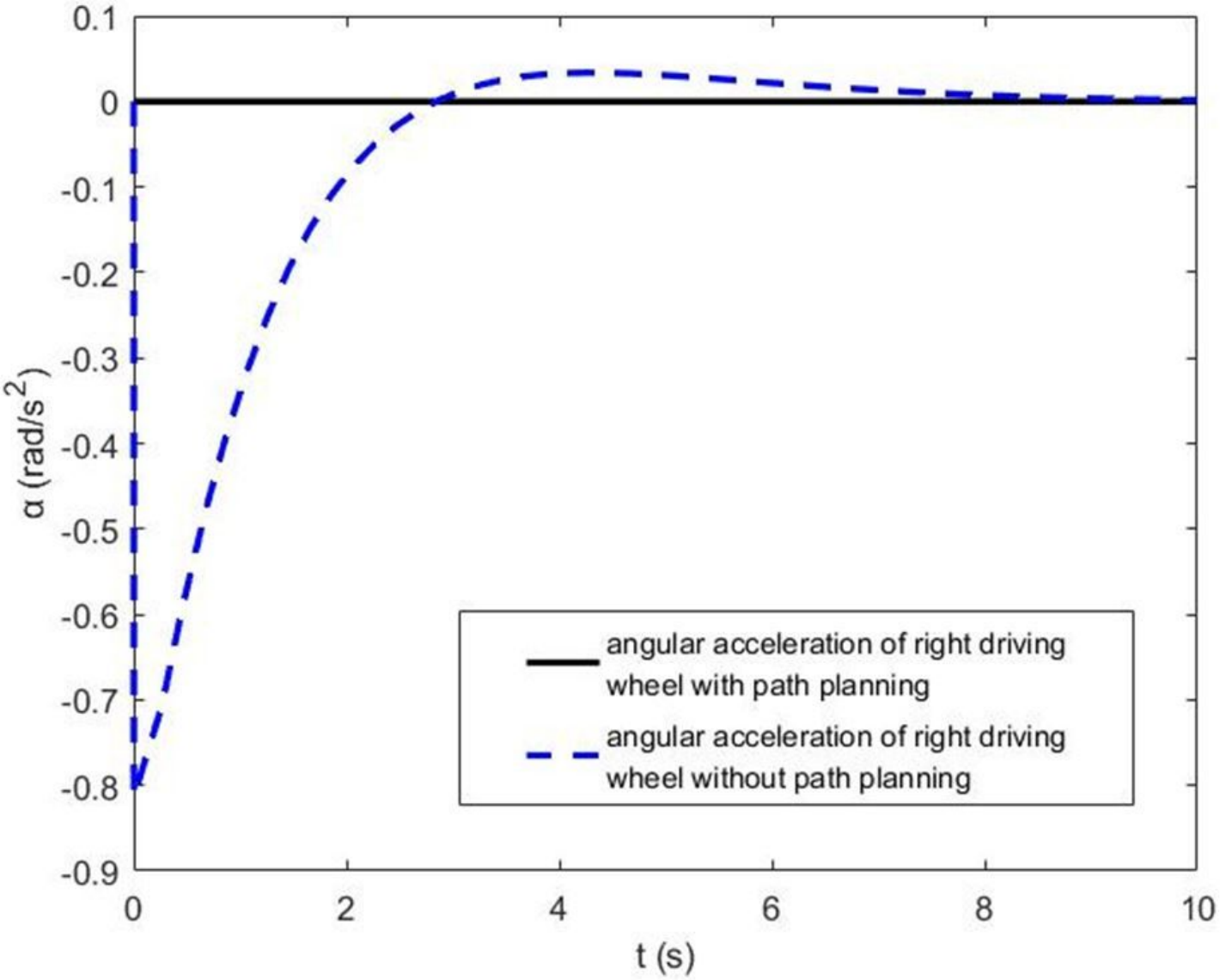

Figure 14

Angular acceleration of right driving wheel

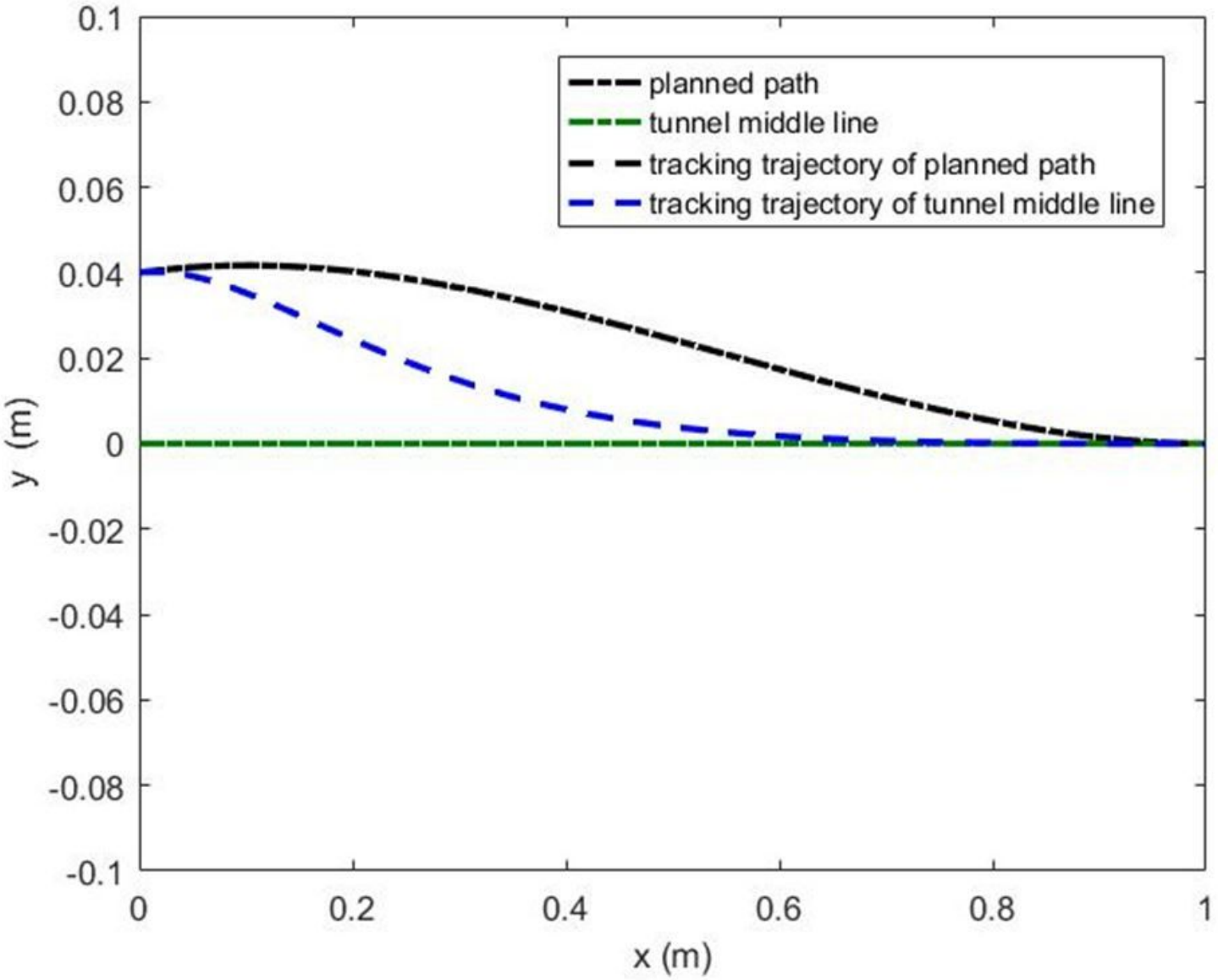

Figure 15

Tracking trajectory of different target paths

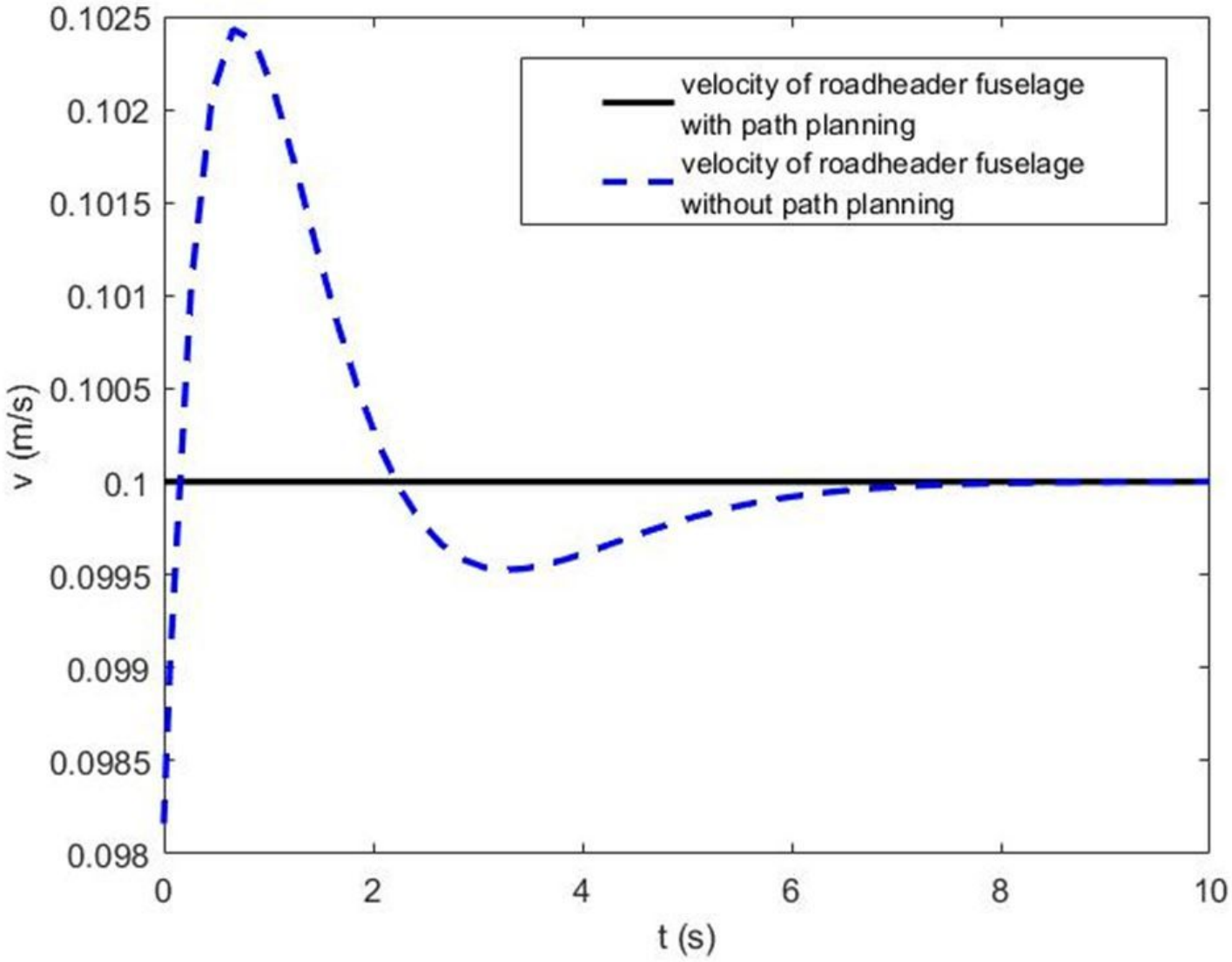

Figure 16

Velocity of roadheader fuselage

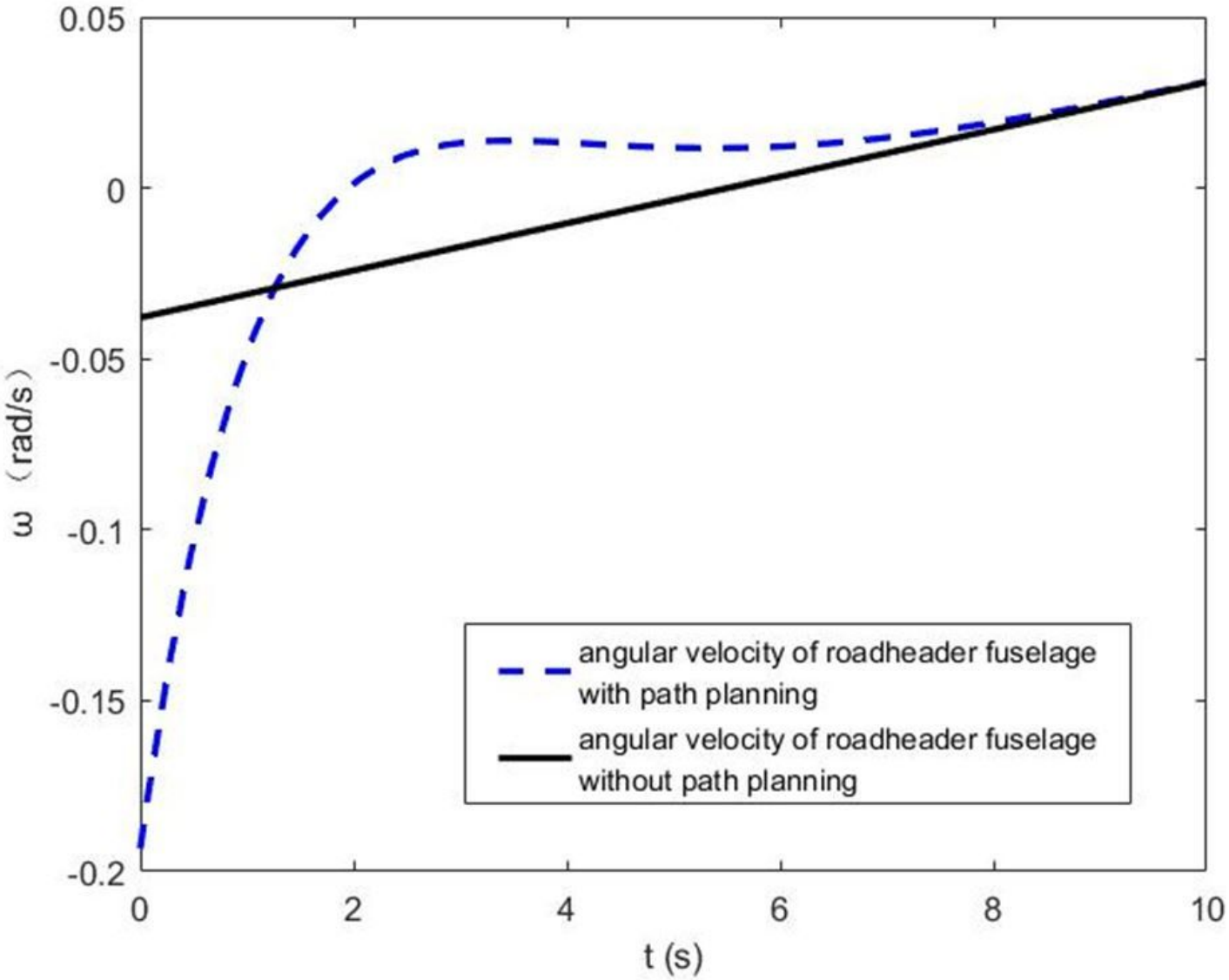

Figure 17

Angular velocity of roadheader fuselage

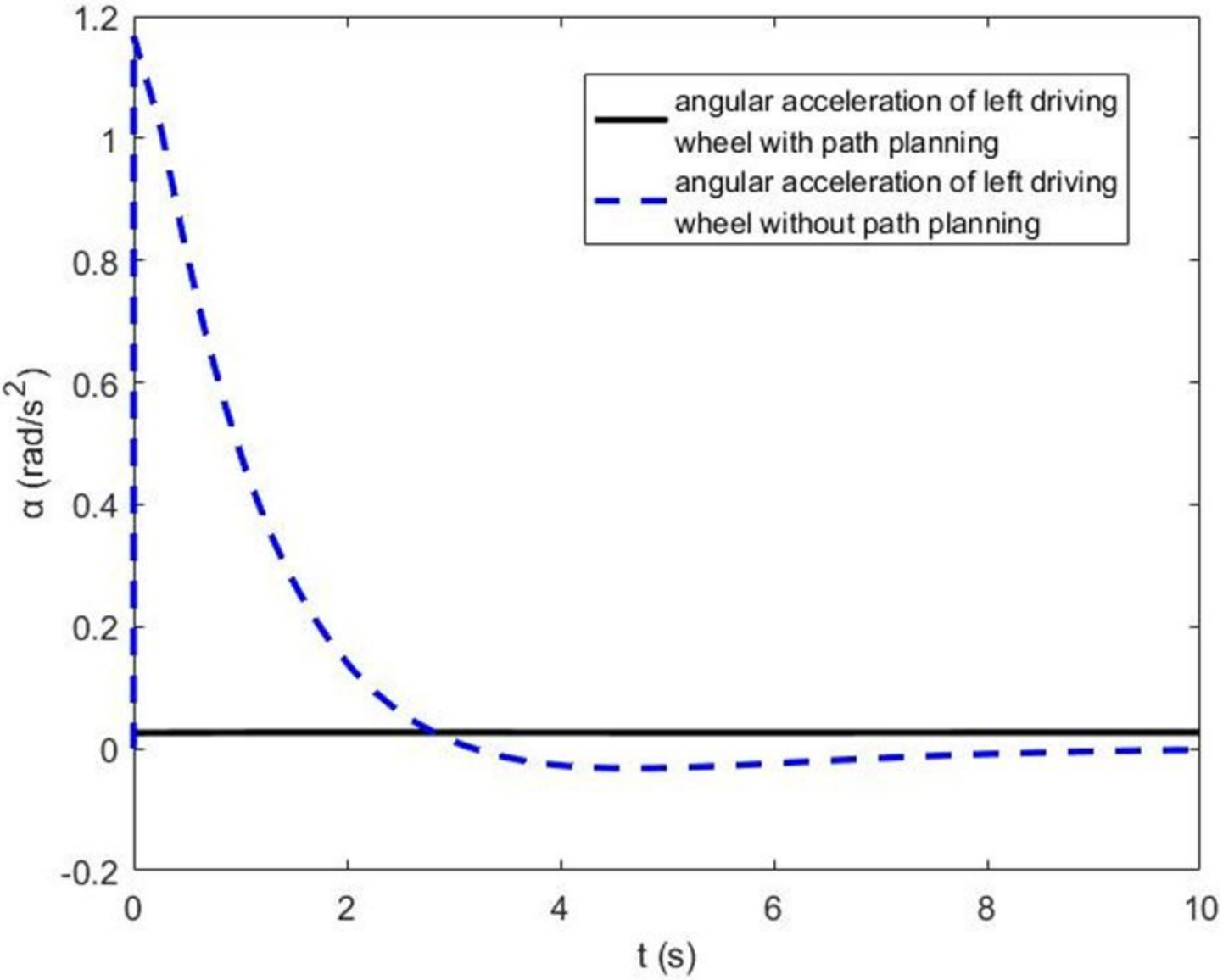

Figure 18

Angular acceleration of left driving wheel

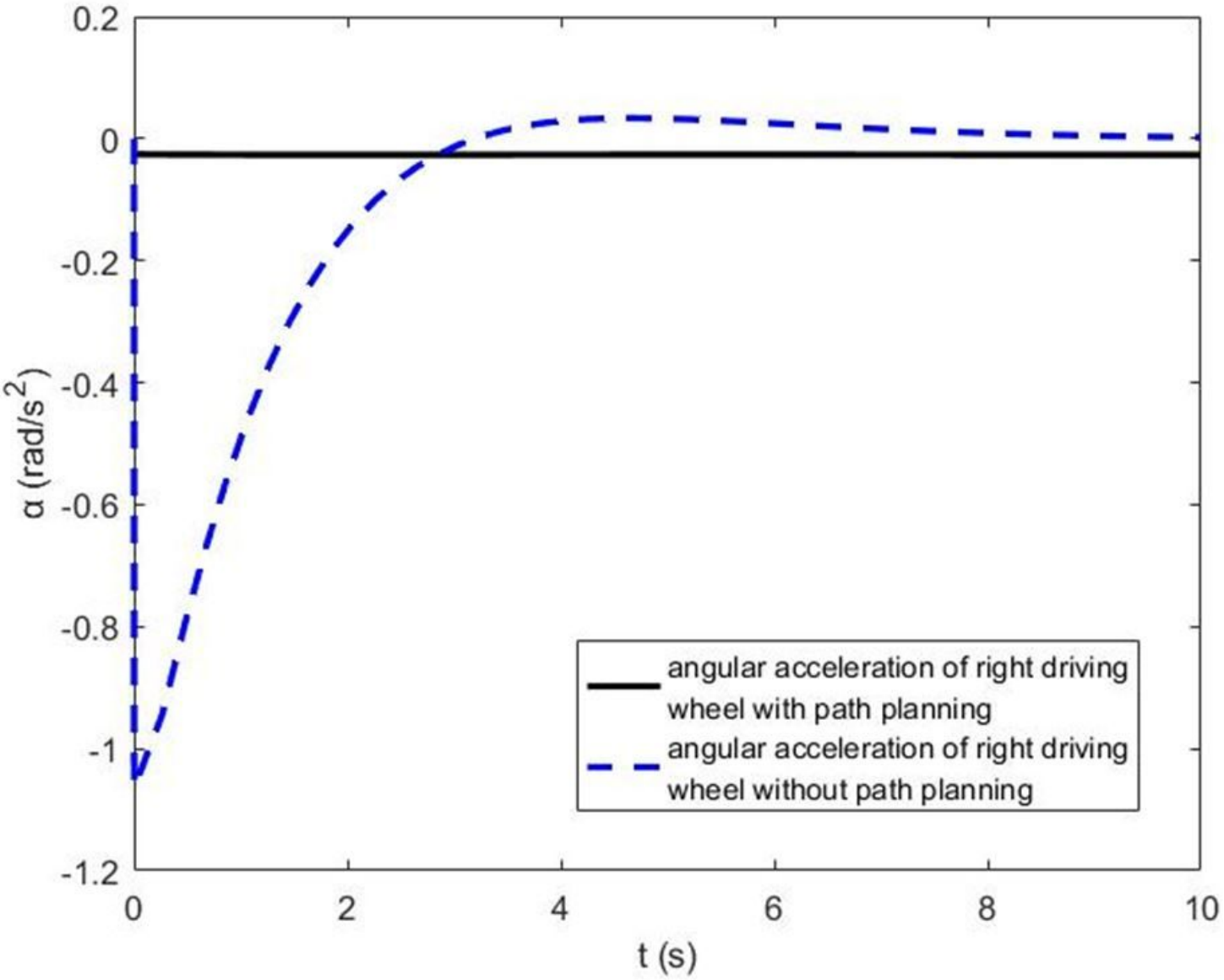

Figure 19

Angular acceleration of right driving wheel